

plant and soil data from continuously active volcanic locations such as Iceland and Hawaii (7). More common values in both of these locations would be one or two orders of magnitude higher.

In general, mercury content of plants is high when mercury content of the soils is also high, but this relation does not always hold. The mercury content of the substratum in both the Kelso and Horsethief Lake regions of Washington, for example, is about 15 ppb, but the mercury content of the plants at Kelso is about 6 ppb and that at Horsethief Lake is about 9 ppb. In some instances, such as at Kelso, the mercury content of plants is less than that of the substrate; in other places, such as at Yakima and Toppenish, the plants contain higher concentrations than the substrate. The variations probably arise from differences in the relative availability to the plant of mercury in the substratum and in the plume ash.

The plants we sampled were, on the average, 10 cm or less in height and less than 6 months in age, yet they reflected with reasonable accuracy the direction of a volcanic plume generated during an eruption that took place months before these plants began their growth.

B. Z. SIEGEL

Pacific Biomedical Research Center,
University of Hawaii at Manoa,
Honolulu 96822

S. M. SIEGEL

Department of Botany,
University of Hawaii at Manoa

References and Notes

1. J. B. Pollack, *Science* **211**, 815 (1981).
2. S. Kieffer, *Nature (London)* **291**, 568 (1981).
3. E. Danielsen, *Science* **211**, 819 (1981).
4. E. Inn, J. Vedder, E. Condon, D. O'Hara, *ibid.*, p. 821; T. Vossler, D. Anderson, N. Aras, J. Phelan, W. Zoller, *ibid.*, p. 827.
5. A. Andren and J. Nriagu, *The Global Cycle of Mercury*, J. Nriagu, Ed. (Elsevier/North-Holland, Amsterdam, 1979); J. Connor, *Sci. Total Environ.* **12**, 241 (1979); B. W. Gandrud and A. L. Lazrus, *Science* **211**, 826 (1981); A. Eshleman, S. Siegel, B. Siegel, *Nature (London)* **233**, O. Joensuu, *Science* **172**, 1027 (1971); J. McCarthy, J. Meuschke, W. Ficklin, R. Learned, *U.S. Geol. Surv. Prof. Pap.* **713** (1973), p. 37; B. Siegel and S. Siegel, *Nature (London)* **241**, 526 (1973); S. Siegel and B. Siegel, *Environ. Sci. Technol.* **9**, 473 (1975).
6. B. Siegel and S. Siegel, *Environ. Sci. Technol.* **12**, 1036 (1978); *Geothermal Res. Counc. Trans.* **2**, 596 (1978).
7. J. Barber, W. Beauford, Y. Sheih, *Mercury, Mercurials and Mercaptans*, M. Miller and T. Clarkson, Eds. (Thomas, Springfield, Ill., 1973); D. Ben-Bassat and A. Mayer, *Physiol. Plant.* **38**, 128 (1975); *ibid.* **40**, 157 (1977); *ibid.* **42**, 32 (1978); J. Garty, M. Galun, E. Kessel, *New Phytol.* **82**, 159 (1979); W. Kama and S. Siegel, *Org. Geochem.* **2**, 99 (1980); G. McMurtry, R. Brill, B. Siegel, S. Siegel, *Antarct. J. U.S.* **14**, 206 (1979); B. Siegel and S. Siegel, *Water Air Soil Pollut.* **5**, 335 (1976); in *Biogeochemistry of Mercury in the Environment*, J. Nriagu, Ed. (Elsevier/North-Holland, Amsterdam, 1979), pp. 131-159; S. Siegel and B. Siegel, in *Third Scientific Assembly, International Association of Meteorology and Atmospheric Physics*, Hamburg, West Germany, 17 to 28 August 1981, Abstr. 3.7; S. Siegel, J. Okasako, P. Kaalakea, B. Siegel, *Organ. Geochem.* **2**, 139 (1980); S.

Siegel, N. Puerner, T. Speitel, *Physiol. Plant.* **32**, 174 (1974); S. Siegel, B. Siegel, A. Eshleman, K. Bachmann, *Environ. Biol. Med.* **2**, 81 (1973); S. Siegel, B. Siegel, G. McMurtry, *Water Air Soil Pollut.* **13**, 109 (1980); S. Siegel, B. Siegel, J. Okasako, *ibid.* **15**, 371 (1981); S. Siegel, B. Siegel, N. Puerner, T. Speitel, F. Thorarinnsson, *ibid.* **4**, 9 (1975).

8. B. Siegel and S. Siegel, paper presented at Botanical Society of America symposium, "Bio-

logical Effects of Mount St. Helens Eruption," held at the 62nd annual meeting, AAAS Pacific Division, Eugene, Ore., 14-19 June 1981.

9. S. Siegel and B. Siegel, *Water Air Soil Pollut.* **9**, 113 (1978).
10. J. S. Fruchter *et al.*, *Science* **209**, 1116 (1980).
11. We thank D. N. Siegel, University of Oregon, for his able assistance in the field.

20 October 1981; revised 12 January 1982

Comet Encke: Radar Detection of Nucleus

Abstract. *The nucleus of the periodic comet Encke was detected in November 1980 with the Arecibo Observatory's radar system (wavelength, 12.6 centimeters). The echoes in the one sense of circular polarization received imply a radar cross section of 1.1 ± 0.7 square kilometers. The estimated bandwidth of these echoes combined with an estimate of the rotation vector of Encke yields a radius for the nucleus of $1.5^{+2.3}_{-1.0}$ kilometers. The uncertainties given are dependent primarily on the range of models considered for the comet and for the manner in which its nucleus backscatters radio waves. Should this range prove inadequate, the true value of the radius of the nucleus might lie outside the limits given.*

Comets are widely believed to represent samples of the most primitive material of the solar nebula (1), and their nuclei especially have been the subject of intense study. However, direct study of the nucleus of a comet has been hindered by the difficulty in separating the light reflected by the nucleus from that scattered by the surrounding coma. Apart from a spacecraft mission to a comet, ground-based radar appears to be the only technique available for the di-

rect detection of a nucleus. But such detection is rarely possible because of the combination of the small size of a comet's nucleus and its generally great distance from the earth.

Comet Encke has the shortest orbital period of any known comet ($P_o = 3.3$ years), and has been observed carefully during most of its passages through perihelion since its discovery in 1786. Its orbit has been determined accurately (2), and its nucleus described (3) as an inho-

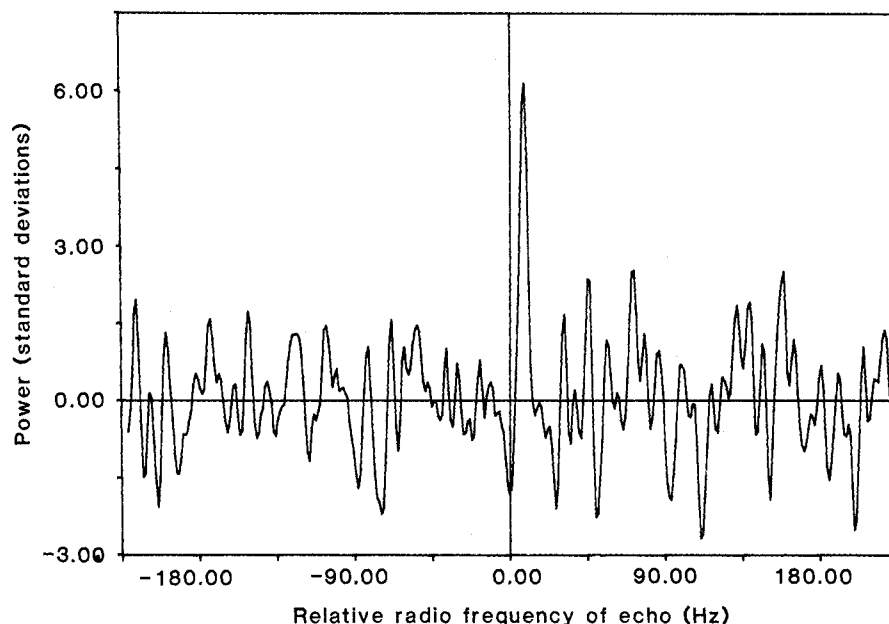


Fig. 1. Smoothed spectrum from radar observations of comet Encke made during the period 2 to 8 November 1980. The abscissa represents the radio frequency of the received signal relative to the frequency calculated from the ephemeris for the comet; the scale spans an interval slightly larger than the smallest difference between any two of the four transmitted frequencies (4). The central peak of the echo is offset by about 7.5 Hz from the ephemeris value which corresponds to the origin of the abscissa. The ordinate represents echo power in units of the root-mean-square fluctuations of the noise power. The distribution of the noise samples in the final spectrum approximates to the expected degree a Gaussian probability distribution of mean zero and standard deviation unity.

mogeneous mixture of ices and meteoroidal material with a radius of about 1.5 km. In November 1980 Encke passed 0.3 AU from the earth, sufficiently close for us to detect radar echoes with the Arecibo Observatory's radar system, operating at a wavelength of 12.6 cm.

Our observations were made on seven consecutive days, from 2 through 8 November 1980, about 1 month before

Encke reached perihelion. Each day's observations were broken into cycles. A cycle consisted of the transmission, for a time approximately equal to the round trip of the echo, of a frequency-switched (4), circularly polarized, nearly monochromatic wave, followed by the reception, for nearly the same duration, of the echo in the sense of circular polarization opposite (OC) to that transmitted. Simul-

taneous reception in both orthogonal senses of circular polarization was not possible at the time of the experiment. Table 1 summarizes the relevant system parameters and shows Encke's geocentric distance. An ephemeris, based on the comet's osculating orbital elements, was used to point the telescope and to adjust the receiver frequency. The received signals were sampled, segmented, Fourier analyzed, corrected for instrumental effects, and combined in groups to obtain power spectra with a frequency resolution of about 1.2 Hz (4). These spectra were then summed to yield a "total" spectrum.

Aside from the effects of noise, this total spectrum is determined by the manner in which the nucleus scatters radio waves. From experience (5) with the probable form of this dependence for both large icy bodies and small rough bodies, we chose a particular parameterized function (6) to approximate the spectral shape of the echo; this function was cross correlated with the total spectrum for various values of the parameters to maximize the signal-to-noise ratio. Figure 1 shows the result of this correlation for a set of parameter values (see below) that yields a maximum signal-to-noise ratio.

Figure 2 shows separately the corresponding spectra for 5 and 6 November and 7 and 8 November after each was correlated with the same function, with the same parameter values, used for Fig. 1. An echo, although not strong, is discernible in each of these spectra and provides powerful evidence that the peaks observed are indeed radar echoes from Encke. In each case, the central peak of the echo is offset by about 7.5 Hz from the value predicted by our ephemeris. However, the optical observations of Encke, including those made both before and after the radar observations, were neither sufficiently numerous nor sufficiently accurate to allow the Doppler shift to be calculated with an uncertainty under 20 Hz, and hence can lend no independent support to this finding of a 7.5-Hz error in the predicted Doppler shift. The measured Doppler shift for the transmitted frequency of 2380 MHz at the epoch 14 hours 44 minutes UT, 5 November 1980, near the midpoint of our observations, is $-280,334.5 \pm 1.0$ Hz (standard error).

The spectrum formed from the observations of 2, 3, and 4 November, after cross correlation with the same function used for the other spectra, yielded a peak at the same frequency offset, but with a lower, 2.5-standard-deviation amplitude.

Table 1. System characteristics for radar observations of periodic comet Encke*

Date (1980)	Δ (AU)	RTT (sec)	G (dB)	P_t (kW)	T_s (K)	t_i (sec)
2 November	0.295	294	69.2	390	79	189
3 November	0.303	302	70.2	300	59	1947
4 November	0.311	310	70.4	345	63	864
5 November	0.321	320	70.6	350	51	3135
6 November	0.332	331	70.8	375	48	3259
7 November	0.343	342	70.8	380	49	3708
8 November	0.355	354	70.8	400	50	3488

* Δ is the geocentric distance of Encke, RTT the round-trip time of the radar signals, G the isotropic antenna gain, P_t the transmitted power, T_s the receiving system temperature, and t_i the integration time of the received signals. The wavelength of the radar signals was 12.6 cm (carrier frequency of 2380 MHz).

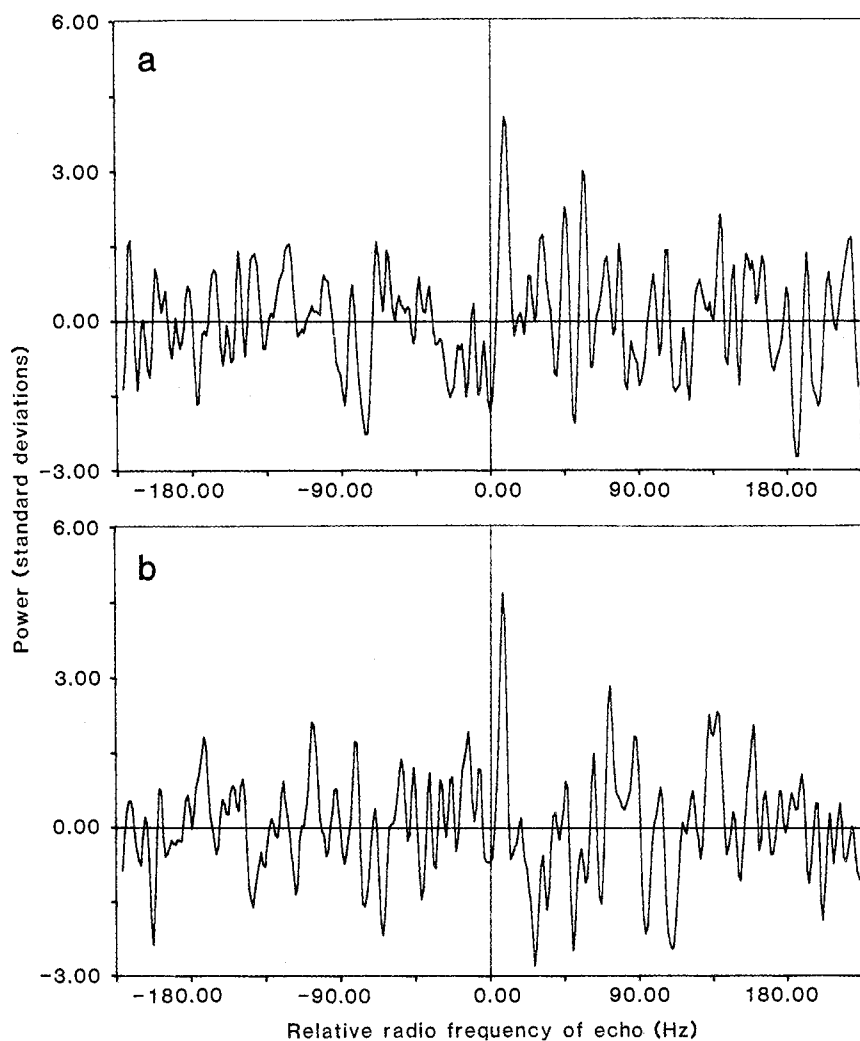


Fig. 2. Smoothed spectra from the data of (a) 5 and 6 November and (b) 7 and 8 November. The frequency corresponding to the central peak of the echo is in each case approximately the same as in Fig. 1.

This difference is due in part to the less sensitive observations made on these earlier days (see Table 1) and perhaps in part to a variability with aspect of the radar reflectivity of Encke's nucleus.

Integration of the total power spectrum over the bandwidth containing the echo yields a radar cross section $\sigma_{OC} = 1.1 \pm 0.7 \text{ km}^2$, where comparable contributions to the estimated standard error come from uncertainties in the calibration of the radar system and from the effects of thermal noise.

To estimate the radius of Encke's nucleus, assumed spherical, we used the relation

$$R = \frac{\lambda B P_s}{8\pi \sin \alpha} 10^{-3} \text{ km}$$

where λ (meters) is the radar wavelength, B (hertz) the total ("limb-to-limb") bandwidth of the echo, P_s (seconds) the spin period of the nucleus, and α the angle between the spin axis and the radar line of sight. The values for B and for the appropriate component of the spin vector of the nucleus must be known to estimate R . The radar echoes allow an estimate to be made only for B . This estimate, however, is seriously affected by its very high correlation with the spectral shape of the echo, which is unknown (7). A further assumption is needed. Assuming a narrow shape, characteristic of specular reflection from a smooth surface, would yield a high value for B , whereas assuming a broad shape, characteristic of a rough surface, would yield a low value. Guided by the shapes inferred from radar observations of asteroids and of the icy Galilean satellites (5), we chose $n = 1.5 \pm 1$ as the value and uncertainty of the exponent of the assumed \cos^{θ} backscattering function (6), the higher values of n implying the narrower shapes. Considering this restriction, and the effect of the other parameters (6), we obtained by least squares the result (8) $B = 6 \pm 3 \text{ Hz}$. The uncertainty is determined primarily by the interval allowed for n ; the statistical standard error (for n fixed) contributes only about 1 Hz to the total. For the rotation vector of Encke, we used the estimates by Whipple and Sekanina (3) obtained from measurements made at various times of halo diameters and coma asymmetries. For a 1980.8 epoch, their results imply that the rotation period is 6 hours 20 minutes \pm 40 minutes (standard error). The ecliptic longitude and latitude of the pole and the associated estimated standard errors are $180^\circ \pm 10^\circ$ and $2^\circ \pm 10^\circ$, respectively (3, 9), where, as for the estimate of B , the

uncertainty in the model assumed for the comet makes the major contribution to the estimated standard error. The corresponding estimates of the radius and its uncertainty for a "worst case" combination of these fractionally large estimated standard errors are given by (8) $R = 1.5^{+2.3}_{-1.0} \text{ km}$. We must emphasize, however, that the errors given represent a worst case only within the limits placed on n and on the comet models that were considered in estimating the rotation vector of Encke. Were we, for example, to broaden the interval of n to encompass $0 \leq n \leq 5$, the corresponding values for B would range from about 2 to 10 Hz and for R from about 0.3 to 4.5 km. By invoking the improbability of a radar cross section that exceeds the geometric cross section and using the lower value of the range for the former, we obtain a similar lower limit of about 0.4 km for the radius of the nucleus.

More radar observations are needed to refine these results and to obtain a detailed description of the reflection properties of the nucleus and their variations over the surface. Unfortunately, comet Encke will not be detectable by radar again until the 1990's. The next possibly useful opportunity for radar detection offered by a periodic comet occurs in 1982, when the comet Grigg-Skjellerup will pass 0.3 AU from the earth. The determination of its radius will again depend on knowledge of the spectral shape of the echo and on the availability of a reliable estimate of its spin vector, which, in turn, will require many careful visual observations (3).

P. G. KAMOUN

Department of Earth and Planetary Sciences, Massachusetts Institute of Technology, Cambridge 02139

D. B. CAMPBELL

National Astronomy and Ionosphere Center, Arecibo, Puerto Rico 00612

S. J. OSTRO

Department of Astronomy, Cornell University, Ithaca, New York 14855

G. H. PETTENGILL

I. I. SHAPIRO

Department of Earth and Planetary Sciences, Massachusetts Institute of Technology

References and Notes

1. F. L. Whipple, in *Cosmic Dust*, J. A. M. McDonnell, Ed. (Wiley, New York, 1978), p. 1.
2. B. G. Marsden, *Catalog of Cometary Orbits* (International Astronomical Union Central Bureau for Astronomical Telegrams, Smithsonian Astrophysical Observatory, Cambridge, Mass., ed. 3, 1979).
3. F. L. Whipple and Z. Sekanina, *Astron. J.* **84**, 1894 (1979).
4. A somewhat elaborate frequency-switching technique was used to remove virtually all in-

strumental effects from the spectra of the received signals. To accomplish this removal, the carrier frequency was switched during transmission in turn among four different values spaced at 448-Hz intervals, dwelling for $T = 10$ seconds at each offset. The received signal, translated to video frequencies with due account for the Doppler shift but not for frequency switching, was separated into 0.82-second segments; each segment was then Fourier-transformed to yield a power spectrum with a resolution of $\sim 1.2 \text{ Hz}$ and a total band of $\sim 2 \text{ kHz}$. (A frequency resolution of 1.2 Hz was chosen because it was easy to implement and appeared adequate to preserve the discernible characteristics of the echo; the spacing of the carrier frequencies was chosen so that the widest conceivable echo broadening could be comfortably accommodated in a band small compared to this spacing; and the total band was set by the need to accommodate the frequency switching.) These spectra, collected for an interval long compared with $T = 10$ seconds, were then summed, the start of each such interval having been delayed from the corresponding start of the transmission by the round-trip time of the echo in order to maintain synchronism with the cycle of frequency switching. Each group of four such summed spectra, corresponding to the four values of the carrier frequency, were then further processed. To clarify the procedures used, we define the quantity S_{ij} ($i, j = 1-4$) to represent each of the four equal quarters j of each of the four spectra i . The echo of each carrier frequency, when present, appears near the center of the corresponding quarter, different for each of the four spectra. Thus if S_{11} contains the echo, then S_{ij} ($j = 2-4$) and S_{i1} ($i = 2-4$) do not. We therefore obtained a "background" spectrum for S_{11} by forming the average

$$(1/3) \sum_{i=2}^4 S_{i1}$$

subtracting it from S_{11} , and dividing the result by it, point by point, to yield a background-free spectrum. In a similar manner the quarter that can contain an echo in each of the other three spectra ($i = 2-4$) was corrected for background, that is, for variations in the spectral response of the radar's receiver system. Using estimates of the root-mean-square of the noise fluctuations, we represented the spectral power in units of the standard deviation of the noise, as in the figures. After this removal of instrumental effects and normalization, all of the sets of four spectra from a given night, properly shifted in frequency, were combined. The total spectrum was obtained by summing the spectra from the individual nights of observation. A more detailed description of this method for removal of instrumental effects is given by Ostro *et al.* (5).

5. D. B. Campbell, J. F. Chandler, G. H. Pettengill, I. I. Shapiro, *Science* **196**, 650 (1977); S. J. Ostro, D. B. Campbell, G. H. Pettengill, I. I. Shapiro, *Icarus* **44**, 431 (1980); R. F. Jurgens and R. M. Goldstein, *ibid.* **28**, 1 (1976).
6. The pattern of radio waves backscattered from "hard" solar system bodies is usually well described by a \cos^{θ} function (5), where θ is the angle of incidence of the wave to the mean spherical surface of the body. (Note that $n = 2$ corresponds to Lambert scattering.) This angular behavior yields an echo whose frequency dependence f can be represented as $A\{1 - [2(f - f_0)/B]^2\}^{n/2}$, where A is the maximum amplitude of the echo, B is the total bandwidth of the echo, and f_0 represents the offset of the center of the spectrum of the echo from the prediction based on the ephemeris.
7. This high correlation is relatively unimportant in determining the radar cross section, since the estimate of the total power received is insensitive to the spectral shape of the echo.
8. A detailed discussion of this determination will be given in the doctoral dissertation of one of us (P.G.K.).
9. Z. Sekanina, personal communication.
10. We are grateful to the staff of the Arecibo Observatory for its assistance with the observations. Special thanks are due to B. Marsden for providing the orbital elements for Encke, to A. Forni for her preparation of the ephemeris, and to P. Ford for assistance with the software. This research has been supported in part by NASA grant NGR 22-002-672 and NSF grant PHY 78-07760. The National Astronomy and Ionosphere Center is operated by Cornell University under contract with the National Science Foundation and with support from the National Aeronautics and Space Administration.

13 November 1981